Cluster mean-field approximations with the coherent-anomaly-method analysis for the driven pair contact process with diffusion

Su-Chan Park and Hyunggyu Park
School of Physics, Korea Institute for Advanced Study, Seoul 130-722, Korea
(Received 6 September 2004; published 26 January 2005)

The cluster mean-field approximations are performed, up to 13 cluster sizes, to study the critical behavior of the driven pair contact process with diffusion (DPCPD) and its precedent, the PCPD in one dimension. Critical points are estimated by extrapolating our data to the infinite cluster size limit, which are in good accordance with recent simulation results. Within the cluster mean-field approximation scheme, the PCPD and the DPCPD share the same mean-field critical behavior. The application of the coherent anomaly method, however, shows that the two models develop different coherent anomalies, which lead to different true critical scaling. The values of the critical exponents for the particle density, the pair density, the correlation length, and the relaxation time are fairly well estimated for the DPCPD. These results support and complement our recent simulation results for the DPCPD.

DOI: 10.1103/PhysRevE.71.016137 PACS number(s): 05.70.Ln, 02.60.−x, 64.60.Ht

The absorbing phase transition (APT) has been studied extensively to understand many-body cooperative phenomena in nonequilibrium systems [1]. Up to now, two universality classes have been firmly established: directed percolation (DP) and parity conservation (PC) universality classes [2]. A few other candidates for different universality classes have been reported in recent literatures. One is the DP system coupled with a static conserved field [3]. Although the reported values for the critical indices are rather scattered [4–6], it is widely believed that these systems form a universality class, different from the DP and the PC class. Another candidate is the pair contact process with diffusion (PCPD) that has as yet defied any consensus on the universality issue. Various scenarios have been proposed, including a new single universality class [7,8], a marginally perturbed DP process with continuously varying exponents [9], and a DP process with a huge crossover time [10,11], which are summarized in a recent review [12].

Recently, we studied the driven PCPD (DPCPD) which is a variant of the PCPD by introducing biased diffusion [13]. It is shown that the driving is relevant and the DPCPD exhibits a "mean-field-like" critical behavior even in one dimension. Since the DP class is insensitive to the driving, the DP scenario with a huge crossover time should be eliminated. There was a recent attempt to understand the PCPD using the renormalization group (RG) analysis on a single-species Bosonic action derived from the microscopic master equation. However, it turned out to be improper to describe the critical behavior of the PCPD [14]. In our previous work [13], we pointed out a possible reason for this failure and suggested that the PCPD may be described properly by a field theory with two independent fields. Still, the search for the coarse-grained action adequate for the PCPD remains a challenge.

Besides the RG technique on the proper action [15], there are a few other efficient methods to investigate the absorbing critical phenomena. Numerical simulations along with a finite-size-scaling analysis [16] and direct integrations of corresponding Langevin equations [17] are two typical examples. Another frequently used method is the cluster mean-field (CMF) approximation [18] followed by the coherent-anomaly method (CAM) analysis [19]. This method is known to be effective to obtain a quantitative phase diagram and sometimes even explore a true critical scaling behavior [20]. However, the accurate measurement of critical indices is only limited to rather simple DP systems. More complex critical behaviors like in the PC and the PCPD classes could not have been probed with a reasonable accuracy as yet by the CAM analysis [21,22].

In this paper, motivated by our recent results that the DPCPD exhibits a distinct critical behavior from the PCPD and also a mean-field-like behavior even in one dimension [13], we develop the CMF approximations for the DPCPD and the PCPD, expecting that the CAM analysis would produce a reasonable estimate for the mean-field-like critical indices of the DPCPD. Also, direct comparison of the CMF data for two models may provide an independent support for different scaling behaviors.

We set up dynamic CMF equations up to $n=13$ cluster size. The steady-state solutions are obtained within machine accuracy using MATHEMATICA. Dynamic information is also extracted from the smallest eigenvalue of the "linearized" transition matrix. Subsequently, through the CAM analysis, we estimate the values of the critical exponents for the particle density, the pair density, the correlation length, and the relaxation time.

The model is defined on a one-dimensional lattice of L sites with periodic boundary conditions. At each site, there is at most one particle and no multiple occupancy is allowed. Hence the configuration is specified by the occupation number which is either 1 or 0 at every site. Each particle hops to the right (left) with transition rate D_R (D_L). The total number of particles in the system varies by branching and annihilating events mediated by a particle pair ($2A \to 3A$ and $2A \to \emptyset$). The transition rate is p $(1-p)$ for the annihilating (branching) event with $0 \leqslant p \leqslant 1$. These three dynamics can be described by the master equation which takes the form

$$\frac{\partial}{\partial t}|P;t\rangle = -\hat{H}|P;t\rangle, \tag{1}$$

where $|P;t\rangle$ is the state vector at time t and the "Hamiltonian" is written as $\hat{H}=\Sigma_{i=1}^{L}\hat{H}_i$ with

$$\hat{H}_i = D_R(\hat{\rho}_i\hat{v}_{i+1} - \hat{a}_i\hat{a}_{i+1}^{\dagger}) + D_L(\hat{v}_i\hat{\rho}_{i+1} - \hat{a}_i^{\dagger}\hat{a}_{i+1}) - p(\hat{a}_i\hat{a}_{i+1} - \hat{\rho}_i\hat{\rho}_{i+1}) - \frac{1-p}{2}(\hat{a}_{i-1}^{\dagger} + \hat{a}_{i+2}^{\dagger} - \hat{v}_{i-1} - \hat{v}_{i+2})\hat{\rho}_i\hat{\rho}_{i+1}, \tag{2}$$

where $\hat{a}_i(\hat{a}_i^{\dagger})$ is the annihilation (creation) operator of hard core particles, satisfying $\{\hat{a}_i,\hat{a}_j^{\dagger}\}=1$ and $[\hat{a}_i,\hat{a}_j]=[\hat{a}_i,\hat{a}_j^{\dagger}]=0$ for $i\neq j$, $\hat{\rho}_i=\hat{a}_i^{\dagger}\hat{a}_i$ is the number operator, and $\hat{v}_i=1-\hat{\rho}_i$.

Three different cases arise depending on the values of D_R and D_L. The case of $D_R=D_L=0$ represents the pair contact process (PCP) which has infinitely many absorbing states and is known to belong to the DP class at least for static situations [23]. Since the cluster approximations along with the CAM analysis have been already performed for the PCP by several authors previously [24], we skip the analysis of the PCP here. The PCPD corresponds to $D_R=D_L\neq 0$ and the DPCPD corresponds to $D_R\neq D_L$. In what follows, we set $D_R+D_L=1$ for convenience and D_R is chosen to be $1/2$ (1) for the PCPD (DPCPD).

We consider an n-site probability function $P_n(\boldsymbol{\rho};t)$. It is defined as the probability at time t to find an n-site cluster of the configurational state $\boldsymbol{\rho}=(\rho_1,\rho_2,\ldots,\rho_n)$, where an occupational state ρ_i at site i takes either 0 or 1. Tracing out Eq. (1) over occupational states outside the cluster ($\{\rho_i\}$ with $i\leqslant 0$ or $i\geqslant n+1$), one may find a formal exact expression

$$\frac{dP_n(\boldsymbol{\rho};t)}{dt} = \tilde{F}_{\boldsymbol{\rho}}(P_n,P_{n+1},P_{n+2}), \tag{3}$$

where the function $\tilde{F}_{\boldsymbol{\rho}}$ involves the sets of n-, $(n+1)$-, and $(n+2)$-site probability. Notice that P_{n+1} and P_{n+2} terms show up due to the boundary dynamics of the n-site cluster.

As the infinite hierarchy appearing in Eq. (3) is the major obstacle towards analytic treatment, we need an approximation scheme to truncate the hierarchy at finite n. In this paper, we take the so-called $(n+1,n)$ approximations [18], where P_{n+2} and P_{n+1} are expressed in terms of products of P_n's. Then, the rate equations for the n-site cluster probability function become

$$\frac{dP_n(\boldsymbol{\rho};t)}{dt} = F_{\boldsymbol{\rho}}(\{P_n\}), \tag{4}$$

where P_n is now the approximate (mean-field) probability function.

The stationary probability distribution function $P_n^s(\boldsymbol{\rho})$ can be obtained by solving the set of coupled equations $F_{\boldsymbol{\rho}}=0$. For given n, the number of equations and the number of variables are both 2^n, but not all are independent. The translational invariance and the normalization condition guarantee that all $P_n(\boldsymbol{\rho})$ with $\rho_1=0$ can be expressed in a linear combination of $P_n(\boldsymbol{\rho})$'s with $\rho_1=1$. For example, in case of $n=4$, one can easily show that $P_4(0011)=P_3(011)-P_4(1011)=P_2(11)-P_3(111)-P_4(1011)=P_3(110)-P_4(1011)=P_4(1101)+P_4(1100)-P_4(1011)$. The absorbing (vacuum) probability $P_4(0000)$ can be determined by the normalization condition. Hence the DPCPD case has 2^{n-1} independent variables. In case of the PCPD, the left-right symmetry further reduces the number of independent variables, for example, $P_4(1101)=P_4(1011)$ and so on.

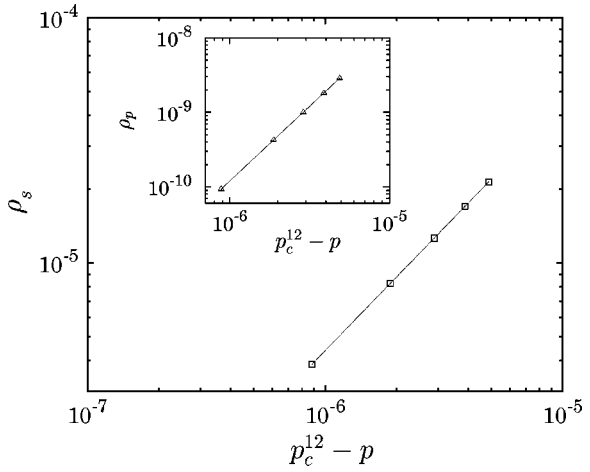

FIG. 1. Log-log plot of ρ_s vs $p_c^{12}-p$ obtained from the 12-cluster CMF approximation for the DPCPD. The slope of the straight line is 1. In the inset, ρ_p's are plotted against $p_c^{12}-p$. The slope of the straight line is 2.

We use MATHEMATICA to find the stationary solutions $P_n^s(\boldsymbol{\rho})$ up to $n=13$ with machine accuracy (10^{-20}) for given values of parameters, p and D_R [25]. With P_n^s, we calculate the particle density ρ_s and the pair density ρ_p in the steady state as

$$\rho_s = P_1^s(1) = \mathrm{Tr}_{\boldsymbol{\rho}}P_n^s(\boldsymbol{\rho})\,\delta_{\rho_k,1},$$

$$\rho_p = P_2^s(11) = \mathrm{Tr}_{\boldsymbol{\rho}}\,P_n^s(\boldsymbol{\rho})\,\delta_{\rho_k,1}\delta_{\rho_{k+1},1}, \tag{5}$$

where k (and $k+1$) denotes an arbitrary site inside the cluster. At a fixed value of D_R, the order parameters, ρ_s and ρ_p, simultaneously vanish for large p (pair annihilation rate) and the system exhibits an absorbing phase transition into vacuum at $p=p_c^n$.

Near the transition point p_c^n, the order parameters scale as

$$\rho_s \simeq A_n(p_c^n-p)^{\beta_1^{\mathrm{MF}}}, \quad \rho_p \simeq B_n(p_c^n-p)^{\beta_2^{\mathrm{MF}}}, \tag{6}$$

where we find the mean-field values for the order parameter exponents: $\beta_1^{\mathrm{MF}}=1$ and $\beta_2^{\mathrm{MF}}=2$. Figure 1 shows the $n=12$ cluster approximation results for the DPCPD. We estimate the critical point p_c^n and the critical amplitudes A_n and B_n by fitting five data near the transition ($|p-p_c^n|\leqslant 5\times 10^{-6}$), linearly for ρ_s and quadratically for ρ_p. Our results are tabulated in Table I for the PCPD model and in Table II for the DPCPD model. Notice that the relative errors for p_c^n are extremely small ($\sim 10^{-9}$), but the amplitudes A_n and B_n still have a sizable relative error ($\sim 10^{-4}$).

It is interesting to note that, for $n\leqslant 3$, the diffusion bias does not enter the CMF rate equations at all. The functional form of $F_{\boldsymbol{\rho}}(\{P_n\})$ in Eq. (4) is identical for the PCPD and the

TABLE I. Cluster approximation results for the PCPD model. The errors are in the last digits.

n	p_c^n	A_n	B_n	C_n
4	0.209 692 7263	4.473	51.855	17.59
5	0.194 357 9912	4.720	72.928	19.15
6	0.184 167 8676	4.859	93.789	19.93
7	0.177 119 7696	4.963	116.26	20.66
8	0.171 815 3824	5.039	139.91	21.22
9	0.167 700 6591	5.100	165.04	21.72
10	0.164 396 9333	5.151	191.63	22.17
11	0.161 685 1815	5.194	219.71	22.58
12	0.159 416 2244	5.232	249.28	22.96
13	0.157 488 7140	5.265	280.35	

DPCPD. The left-right symmetry among $P_n(\boldsymbol{\rho})$'s is automatically enforced due to the translational invariance, regardless of the details of the dynamics. For example, $P_3(110) = P_2(11) - P_3(111) = P_3(011)$ and so on. However, for $n \geqslant 4$, the translational invariance does not guarantee the left-right symmetry, which may be broken by the dynamics with a broken left-right symmetry.

In nonequilibrium systems, dynamic relaxation behavior provides one of the key pieces of information on the system. Off criticality, the order parameters are expected to approach their stationary values exponentially with a characteristic relaxation time τ. At criticality, τ diverges and the order parameters decay algebraically. One may roughly estimate τ by numerically integrating the rate equations (4) and fitting time-dependent data into an exponential form. However, this method does not produce high-precision data. In this paper, we propose a different method to calculate τ with machine accuracy in the CMF approximation scheme.

Since the stationary solutions of Eq. (4) were obtained with machine accuracy, we can linearize Eq. (4) near the stationary solutions very accurately. The linearized equation takes the form

TABLE II. Cluster approximation results for the DPCPD model. The errors are in the last digits.

n	p_c^n	A_n	B_n	C_n
4	0.216 140 3513	4.254	44.37	16.69
5	0.202 800 9465	4.356	56.08	17.31
6	0.194 381 7410	4.405	66.48	17.55
7	0.188 503 1907	4.423	76.39	17.74
8	0.184 102 4774	4.424	85.76	17.83
9	0.180 689 8311	4.420	94.89	17.90
10	0.177 954 3360	4.410	103.7	17.94
11	0.175 711 7674	4.397	112.3	17.97
12	0.173 837 8803	4.383	120.8	17.99
13	0.172 247 8976	4.368	128.9	

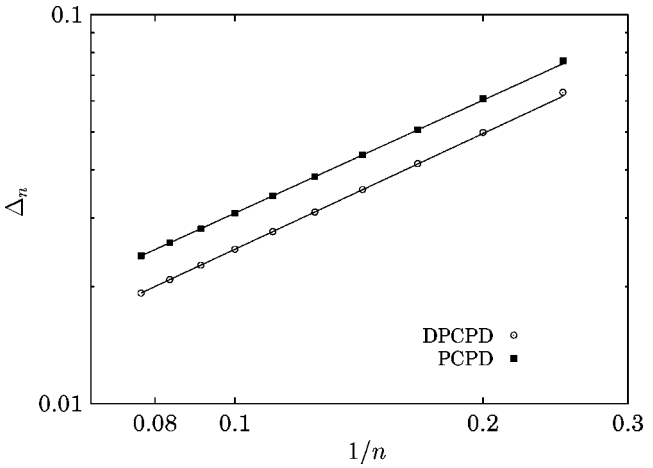

FIG. 2. Log-log plots of Δ_n vs $1/n$ for the PCPD and the DPCPD. In this figure, the value of p_c for the PCPD (DPCPD) is set to be 0.1335 (0.153).

$$\frac{d|P_n;t\rangle}{dt} = -\boldsymbol{M}|P_n;t\rangle, \tag{7}$$

where $|P_n;t\rangle$ is the (n-cluster) state vector with the components $P_n(\boldsymbol{\rho};t)$ and $\boldsymbol{M}$ is a square matrix. It is trivial to show that the eigenvalues of $\boldsymbol{M}$ are equal to the inverse of various characteristic time scales of the dynamics. The most dominant slow mode is determined by the smallest eigenvalue Λ_s, i.e., the relaxation time $\tau = \Lambda_s^{-1}$.

We analyze the linearized equation up to $n=12$. Near criticality, we find

$$\tau^{-1} \simeq C_n (p_c^n - p)^{\nu_\parallel^{\mathrm{MF}}}, \tag{8}$$

where we find again the mean-field value for the relaxation exponent, $\nu_\parallel^{\mathrm{MF}} = 2$. We estimate the critical points p_c^n independently, which are found to be consistent with previous estimates from the density data in Tables I and II, where we also tabulate the estimated values for the amplitude C_n for both the PCPD and the DPCPD.

Now, we employ the coherent-anomaly method (CAM) introduced by Suzuki and co-workers [19] and estimate the values of the true critical exponents. Following the CAM analysis, the n dependence of the critical point p_c^n is predicted in the large n limit as

$$\Delta_n^{\nu_\perp} \sim n^{-1}, \tag{9}$$

where $\Delta_n = p_c^n - p_c$ is the distance of p_c^n from the true critical point $p_c = \lim_{n\to\infty} p_c^n$ and $\nu_\perp$ is the true correlation length exponent.

We estimate p_c by applying the Bulirsch and Stoer (or BST) algorithm [26] to the series of $\{p_c^n\}$ and find that $p_c = 0.134(2)$ for the PCPD and $p_c = 0.154(3)$ for the DPCPD, which are in good agreement with simulation results of 0.133 522(2) and 0.151 032(1) [13]. Alternatively, we estimate p_c and $\nu_\perp$ simultaneously using Eq. (9). In Fig. 2, we plot Δ_n vs $1/n$ in a log-log plot, varying p_c to find the best power-law fit. For the PCPD, the choice of $p_c = 0.1335$ yields the smallest fitting error with $\nu_\perp = 1.04$, where the data from $n=8$ to

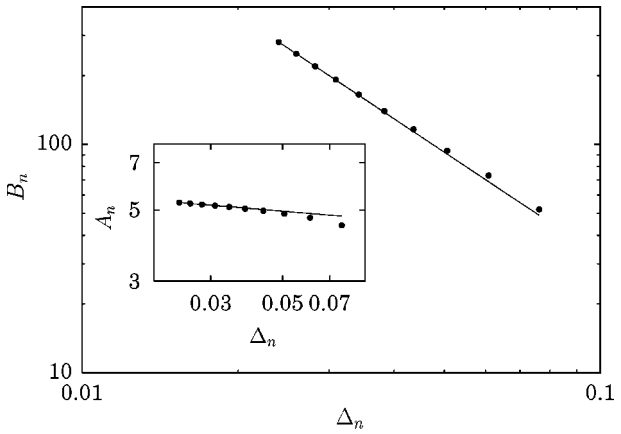

FIG. 3. The CAM analysis for the order parameters for the PCPD model. The slope of the straight line is −1.51, which leads to $\beta_2 \approx 0.49$. In the inset, the slope of the straight line is −0.084, which leads to $\beta_1 \approx 0.92$.

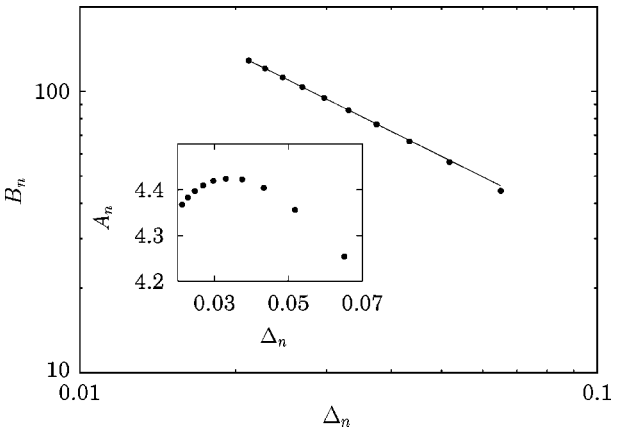

FIG. 4. The CAM analysis for the order parameters for the DPCPD model. The slope of the straight line is −0.92, which leads to $\beta_2 \approx 1.08$. In the inset, A_n vs Δ_n is drawn without a log scale A_n remains nearly constant which implies $\beta_1 \approx \beta_1^{\mathrm{MF}} = 1$.

13 are used. For the DPCPD, the best choice is $p_c = 0.153$ with $\nu_\perp = 1.01$. The relative error for p_c is ∼2%, and the error for $\nu_\perp$ is ∼10%. The best simulation result of $\nu_\perp = 1.09(2)$ for the PCPD is within the errors, but the accurate measurement seems to be out of reach with data up to $n = 13$. Our estimate of $\nu_\perp = 1.01$ for the DPCPD is in very good agreement with the expected mean-field value $\nu_\perp^{\mathrm{MF}} = 1$.

The amplitudes A_n and B_n are expected to scale as

$$A_n \sim \Delta_n^{-(\beta_1^{\mathrm{MF}} - \beta_1)}, \quad B_n \sim \Delta_n^{-(\beta_2^{\mathrm{MF}} - \beta_2)}, \tag{10}$$

where β_1 and β_2 are the true critical exponents for the order parameters. In Fig. 3, the log-log plots of A_n and B_n vs Δ_n for the PCPD are presented. Here we use $p_c = 0.133\,522$ (the best estimate from Monte Carlo simulations) [13]. The CAM analysis leads to $\beta_1 \approx 0.92$ and $\beta_2 \approx 0.49$ [27], both of which are far from the simulation results of $\beta_1 \approx \beta_2 \approx 0.36(2)$ [8,9]. In particular, there is a huge discrepancy between the estimated values of β_1 and β_2 by the CAM analysis, which warns us that the CAM estimates for the order parameter exponents should be interpreted with great caution. This huge discrepancy also implies that the cluster sizes up to $n = 13$ are still too small for the PCPD to reach the asymptotic regime where the system is dominated by long spatial correlations, induced by the long-term memory mediated by solitary particles [9].

On the other hand, the CAM analysis for the DPCPD looks consistent with the simulation results. In Fig. 4, we use $p_c = 0.151\,032$ [13]. First, A_n seems not diverging as $\Delta_n \to 0$ and reaching a nonzero constant, which implies $\beta_1 = \beta_1^{\mathrm{MF}} = 1$. Second, B_n behaves very differently from A_n and diverges with the exponent ∼0.92, which implies that $\beta_2 = \beta_2^{\mathrm{MF}} - 0.92 \approx 1.08$. Numerical simulation results [13] are in complete agreement with our CAM results. One should notice that β_2 does not assume the MF value, but seems to be equal to β_1 except a probable multiplicative logarithmic correction as found in the exponent $\beta/\nu_\parallel$ by numerical simulations [13]. This mean-field-like behavior is expected for the two-dimensional PCPD [28], of which the upper critical dimension is believed to be 2. Our CAM results independently support the conclusion drawn from our numerical simulations results [13] that the DPCPD critical behavior is distinct from the PCPD behavior and the upper critical dimension for the DPCPD is 1 rather than 2.

Finally, we estimate $\nu_\parallel$ from the relation

$$C_n \sim \Delta_n^{-(\nu_\parallel^{\mathrm{MF}} - \nu_\parallel)}, \tag{11}$$

where $\nu_\parallel$ is the true critical exponent for the relaxation time. In Fig. 5, the log-log plots of C_n vs Δ_n are shown. We estimate that $\nu_\parallel \approx 1.8$ for the PCPD and $\nu_\parallel \approx 1.98$ for the DPCPD. Rather surprisingly, the PCPD result is consistent with the simulation result of $\nu_\parallel = 1.85(10)$ [8,9]. For the DPCPD, the value of $\nu_\parallel$ is quite close to the mean-field value of $\nu_\parallel^{\mathrm{MF}} = 2$, consistent with the simulation results.

In summary, we estimated the critical exponents for the PCPD and the DPCPD, using CMF approximations along with the CAM analysis. For the PCPD, the values of the

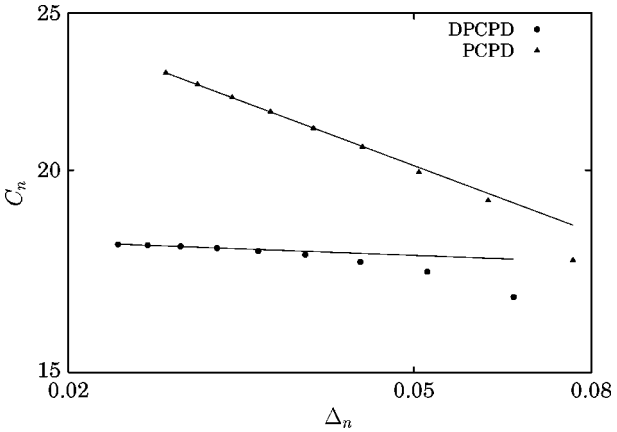

FIG. 5. The CAM analysis for the relaxation time for the PCPD and the DPCPD. The slope of the straight line for the PCPD (DPCP) is −0.2 (−0.02) which leads to $\nu_\parallel = 1.8$ (1.98).

order parameter exponents are poorly estimated, while the estimates for the correlation and the relaxation exponents are consistent with simulation results within error bars. In contrast, the CAM estimates for the DPCPD are in excellent accord with simulation results, supporting our conjecture that the upper critical dimension of the DPCPD is 1.

[1] J. Marro and R. Dickman, *Nonequilibrium Phase Transitions in Lattice Models* (Cambridge University Press, Cambridge, England, 1999).

[2] For a review, see, e.g., H. Hinrichsen, Adv. Phys. **49**, 815 (2000).

[3] M. Rossi, R. Pastor-Satorras, and A. Vespignani, Phys. Rev. Lett. **85**, 1803 (2000).

[4] J. Kockelkoren and H. Chaté, e-print cond-mat/0306039.

[5] S.-C. Park and H. Park (unpublished).

[6] H. Chaté (private communication).

[7] H. Hinrichsen, Phys. Rev. E **63**, 036102 (2001); Physica A **291**, 275 (2001); K. Park and I.-M. Kim, Phys. Rev. E **66**, 027106 (2002).

[8] J. Kockelkoren and H. Chaté, Phys. Rev. Lett. **90**, 125701 (2003).

[9] J. D. Noh and H. Park, Phys. Rev. E **69**, 016122 (2004).

[10] H. Hinrichsen, Physica A **320**, 249 (2003).

[11] G. T. Barkema and E. Carlon, Phys. Rev. E **68**, 036113 (2003).

[12] M. Henkel and H. Hinrichsen, J. Phys. A **37**, R117 (2004).

[13] S.-C. Park and H. Park, e-print cond-mat/0406606.

[14] H.-K. Janssen, F. van Wijland, O. Deloubriere, and U. C. Täuber, Phys. Rev. E **70**, 056114 (2004).

[15] M. Doi, J. Phys. A **9**, 1465 (1976); **9**, 1479 (1976); P. Grassberger and M. Scheunert, Fortschr. Phys. **28**, 547 (1980); L. Peliti, J. Phys. (Paris) **46**, 1469 (1985); B. P. Lee, J. Phys. A **27**, 2633 (1994); J. L. Cardy and U. C. Täuber, J. Stat. Phys. **90**, 1 (1998).

[16] T. Aukrust, D. A. Browne, and I. Webman, Phys. Rev. A **41**, 5294 (1990).

[17] I. Dornic, H. Chaté, and M. A. Muñoz, e-print cond-mat/0404105.

[18] D. ben-Avraham and J. Köhler, Phys. Rev. A **45**, 8358 (1992).

[19] M. Suzuki and M. Katori, J. Phys. Soc. Jpn. **55**, 1 (1986); M. Suzuki, *ibid.* **55**, 4205 (1987); J. Stat. Phys. **49**, 977 (1987).

[20] H. Park, J. Köhler, I.-M. Kim, D. ben-Avraham, and S. Redner, J. Phys. A **26**, 2071 (1993); A. L. C. Ferreira and S. K. Mendiratta, *ibid.* **26**, L145 (1993); N. Inui, Phys. Lett. A **184**, 79 (1993).

[21] N. Menyhárd and G. Ódor, J. Phys. A **28**, 4505 (1995).

[22] A. Szolnoki, e-print cond-mat/0408114.

[23] I. Jensen, Phys. Rev. Lett. **70**, 1465 (1993).

[24] R. Dickman, W. R. M. Rabêlo, and G. Ódor, Phys. Rev. E **65**, 016118 (2001); A. Szolonoki, *ibid.* **66**, 057102 (2002).

[25] The conventional numerical integration methods allow us to find approximate solutions for larger n [22], but the accuracy is much more limited ($\sim 10^{-10}$) within a reasonable computing time.

[26] R. Bulirsch and J. Stoer, Numer. Math. **6**, 413 (1964); M. Henkel and G. Schütz, J. Phys. A **21**, 2617 (1988).

[27] The value of β_2 was independently reported by Szolnoki [22] very recently in the CMF scheme with the CAM analysis.

[28] G. Ódor, M. C. Marques, and M. A. Santos, Phys. Rev. E **65**, 056113 (2002); S.-C. Park and H. Park (unpublished).